Kalai–Smorodinsky Bargaining Solution for Optimal Resource Allocation over Wireless DS–CDMA Visual Sensor Networks

Katerina Pandremmenou, Lisimachos P. Kondi, and Konstantinos E. Parsopoulos

Department of Computer Science, University of Ioannina, GR–45110 Ioannina, Greece

ABSTRACT

Surveillance applications usually require high levels of video quality, resulting in high power consumption. The existence of a well–behaved scheme to balance video quality and power consumption is crucial for the system's performance. In the present work, we adopt the game–theoretic approach of Kalai–Smorodinsky Bargaining Solution (KSBS) to deal with the problem of optimal resource allocation in a multi–node wireless visual sensor network (VSN). In our setting, the Direct Sequence Code Division Multiple Access (DS–CDMA) method is used for channel access, while a cross–layer optimization design, which employs a central processing server, accounts for the overall system efficacy through all network layers. The task assigned to the central server is the communication with the nodes and the joint determination of their transmission parameters. The KSBS is applied to non–convex utility spaces, efficiently distributing the source coding rate, channel coding rate and transmission powers among the nodes. In the underlying model, the transmission powers assume continuous values, whereas the source and channel coding rates can take only discrete values. Experimental results are reported and discussed to demonstrate the merits of KSBS over competing policies.

Keywords: Visual sensor network, DS–CDMA, cross–layer optimization, resource allocation, Kalai–Smorodinsky bargaining solution, game theory.

1. INTRODUCTION

Nowadays, video surveillance applications are widely used in order to monitor large areas and detect events of interest. Such applications basically aim at the assurance of high image quality levels, especially in scenes with high motion, since these scenes usually contain more important information.

In this paper, we assume that a number of nodes are involved in a wireless visual sensor network (VSN), and each of them can access the network using the direct sequence code division multiple access (DS–CDMA) channel access method. The VSN also consists of a centralized control unit (CCU), which gathers and synchronizes data from the source nodes, coordinating the whole resource allocation process. Specifically, the CCU performs source and channel decoding in order to receive the video from each node, while it is also responsible for possible requests for changes in the transmission parameters of the nodes, according to the needs of each application. Therefore, the CCU is assigned the task of properly adjusting the source coding rates, channel coding rates and transmission powers of all nodes, with the goal of maximizing the video quality that reaches the end–user.

This is precisely the idea behind the cross–layer optimization scheme employed in our approach. The cross–layer design allows all network layers to communicate with each other regardless of their position in the layer hierarchy. Thus, they can exchange information and provide services not only to their upper layers but also to any other layer, if necessary. Also, their received services can originate from any other network layer.[1] All these properties compose a multi–node resource sharing problem, which shall be efficiently addressed to attain the optimal system performance.

The resource sharing problem has been addressed with different approaches. In previous work,[2] we focused on strategies for minimizing either the average or the maximum video distortion among the nodes, utilizing the minimum average distortion (MAD) and the minimum maximum distortion (MMD) criteria, respectively. In another approach, the problem was tackled by using the Nash bargaining solution (NBS).[3] This approach

E-mail: apandrem@cs.uoi.gr (K. Pandremmenou), lkon@cs.uoi.gr (L.P. Kondi), kostasp@cs.uoi.gr (K.E. Parsopoulos)

allowed the optimal allocation of the available system resources, under the assumption of nodes' cooperation. In the present work, we adopt a bargaining strategy from the field of Game Theory, which was proposed by Kalai and Smorodinsky in 1975.[4] In the past, KSBS has been used in different types of resource allocation problems. However, in our approach, the requirement of convex feasible sets is relaxed, according to Ref. 5. Applications of the KSBS in related problems can be found in Refs. 6, 7, 8, 9, 10, 11.

In our experimental configuration, we applied KSBS to a video–quality optimization problem in order to ensure the Quality of Service required by wireless DS–CDMA VSN applications, allowing continuous values for the transmission powers and discrete values for the source and channel coding rates. The obtained results corroborated the efficacy of KSBS in confronting the challenge of optimal resource sharing among different nodes in a wireless DS–CDMA VSN, frequently outperforming the aforementioned methods.

The rest of the paper is organized as follows: in Section 2, the basic features of DS–CDMA VSNs are described, while the expected video distortion is derived in Section 3. Section 4 presents the employed cross–layer technique and Section 5 introduces the necessary concepts from Game Theory. In Sections 6 and 7, the proposed bargaining solution is meticulously investigated and some necessary assumptions are presented. Section 8 reports the experimental results along with performance assessments of the proposed approach. Finally, in Section 9, conclusions are drawn.

2. VISUAL SENSOR NETWORK

The use of the DS–CDMA channel access method allows all nodes to transmit over the same channel, sharing the same bandwidth, at the cost of generated interference among the nodes. Since thermal and background noise are usually negligible compared to the interference, they are not included in our model while interference is approximated by additive white Gaussian noise.[2] The power assigned to each node k is given as:

$$S_k = R_k \, E_k, \tag{1}$$

measured in Watts, with the total bit rate, R_k, being equal to the ratio of the source coding rate, $R_{\mathrm{s},k}$, to the channel coding rate, $R_{\mathrm{c},k}$, i.e.:

$$R_k = \frac{R_{\mathrm{s},k}}{R_{\mathrm{c},k}}, \tag{2}$$

measured in bits–per–second (bps). The quantity E_k in Eq. (1) is the energy–per–bit, while the ratio that describes the energy–per–bit to multiple access interference (MAI) is equal to:

$$\frac{E_k}{N_0} = \frac{\frac{S_k}{R_k}}{\sum\limits_{j \neq k}^{K} \frac{S_j}{W_t}}, \tag{3}$$

where $k = 1, 2, \ldots, K$, denotes the corresponding node; $N_0/2$ is the two–sided noise power spectral density due to MAI, measured in Watts/Hertz; S_k is the power of the node of interest; S_j is the power of interfering node j; and W_t is the total bandwidth, measured in Hertz.

The H.264/AVC video coding standard was employed to compress the video sequences imaged by the nodes, in combination with the High profile for 4:2:0 color format video. For the channel coding, we used rate compatible punctured convolutional (RCPC) codes,[12] which simplify Viterbi decoding and allow the use of Viterbi's upper bounds on the bit error probability, P_{b}, defined as:

$$P_{\mathrm{b}} \leqslant \frac{1}{P} \sum_{d=d_{\mathrm{free}}}^{\infty} c_d P_d, \tag{4}$$

where P is the period of the code; d_{free} is the free distance of the code; c_d is the information error weight; and P_d is the probability that the wrong path at distance d is selected.[12] This is defined as:

$$P_d = \frac{1}{2} \operatorname{erfc}\left(\sqrt{d R_{\mathrm{c}} \frac{E_k}{N_0}} \right), \tag{5}$$

where,

$$\mathrm{erfc(x)} = \frac{2}{\sqrt{\pi}} \int_{\mathrm{x}}^{\infty} \exp\left(-\mathrm{t}^2\right) \mathrm{dt},$$

is the *complementary error function*, while R_{c} is the channel coding rate and E_k/N_0 is the energy–per–bit to MAI ratio, given in Eq. (3), for the corresponding node k of the network.

3. EXPECTED VIDEO DISTORTION

Let $E[D_{\mathrm{s+c},k}]$ denote the expected video distortion for node k, which results from both lossy compression and channel errors. This distortion can be estimated by utilizing *universal rate distortion characteristics* (URDC),[2,3] which express the expected video distortion as a function of the bit error probability, P_{b}, after channel decoding:

$$E[D_{\mathrm{s+c},k}] = \alpha \left[\log_{10}\left(\frac{1}{P_{\mathrm{b}}}\right)\right]^{-\beta}, \tag{6}$$

where α and β are positive parameters, highly dependent on the video content characteristics and the source coding rate. Videos that include high levels of motion are usually characterized by larger values of α. The values of α and β are determined using mean squared error optimization for a number of experimentally determined pairs $(E[D_{s+c,k}], P_{\mathrm{b}})$, following the process described below.

For a given bit error rate, we determine the rate of the packet loss according to the real–time transport protocol. Then, packets are dropped from the examined video bit stream. The corrupted video sequence is then decoded using the H.264/AVC video codec and, finally, the expected video distortion is obtained. Due to the fact that a video transmission is subject to channel noise, channel errors are randomly introduced. For this reason, the same process is repeated 300 times (in our case) and the expected video distortion is averaged over all experiments.

Moreover, we require an additional constraint. Specifically, all nodes are assumed to transmit data with the same total bit rate, R_k, meaning that the source and channel coding rates have to share the same bit rate, as implied by Eq. (2). This means that higher source coding rates are associated with lower channel coding rates and vice versa, since their ratio shall remain constant. Also, given that channel coding rates can take only discrete values,[12] source coding rates shall also be restricted to discrete values.

Considering the aforementioned constraint about the available bit rate, we denote as cb the admissible source–channel coding rate combinations. The parameters α and β of Eq. (6) are defined as functions in the source coding rates, whereas d_{free} and c_d of Eq. (4), are functions in the channel coding rates. Hence, all the aforementioned parameters depend on the source–channel coding rate combinations. Substituting Eqs. (3), (4) and (5) in Eq. (6), it follows that:

$$E[D_{\mathrm{s+c},k}](R_{\mathrm{s},k}, R_{\mathrm{c},k}, S) = \alpha(cb) \left[\log_{10}\left(\frac{1}{P} \sum_{d=d_{\mathrm{free}}(cb)}^{\infty} \left(c_d(cb)\, \frac{1}{2}\, \mathrm{erfc}\left(\sqrt{d\, R_{\mathrm{c},k}\, \frac{S_k/R_k}{\sum_{j\neq k}^{K} S_j/W_t}}\right)\right)\right)^{-1}\right]^{-\beta(cb)}, \tag{7}$$

where $k = 1, 2, \ldots, K$. The above equation expresses the expected video distortion for node k as a function of its source coding rate, $R_{\mathrm{s},k}$, and channel coding rate, $R_{\mathrm{c},k}$, as well as of the transmission powers, $S = (S_1, S_2, \ldots, S_K)^{\top}$, of all nodes.

4. CROSS–LAYER DESIGN

The cross–layer scheme considered in our study allows the different network layers to communicate with each other in order to exchange information even in case of not being adjacent. The use of such a flexible scheme optimizes the end–to–end system's performance, overcoming possible network latency problems.

The cross–layer design assumes that the physical layer, data link layer, network layer and application layer, cooperate with each other, optimizing the overall network performance. At the physical layer, the transmission

powers are determined, while at the data link layer, the optimal channel coding rates are selected. At the top of the hierarchy, i.e., application layer, the compression rates are chosen. The layer collaboration is coordinated by a CCU lying at the network layer, which undertakes to communicate with all nodes in order to request changes in the transmission parameters according to their unique, content–aware needs for resources.

Specifically, if the content of a video is deemed less important, the CCU can request from the node capturing the specific video to transmit the data at a lower picture quality, implying a lower source coding rate. Thus, a higher channel coding rate can be used, providing higher protection to the video during transmission. The nodes that compress the captured scenes at a lower compression rate can afford to use lower transmission power, achieving the dual benefit of energy conservation for the battery–operated cameras as well as interference reduction to the transmissions of the rest of the nodes.

5. GAME–THEORETIC CONCEPTS

Game Theory is the branch of mathematics that attempts to model the collaborative or conflicting behaviors of the players that participate in each considered game, providing useful mathematical tools for this purpose. In the present work, the considered game is the resource allocation problem, while the nodes of the network represent the players of the considered game. In the next paragraphs, we briefly present some basic notions that are necessary for the understanding of our proposed method.

A key concept in a game is the *utility function*, U_k, which constitutes a measure of relative satisfaction for each node k of the network. In our problem, the utility function is defined with the peak signal to noise ratio (PSNR), namely:

$$U_k = 10 \log_{10} \frac{255^2}{E[D_{\mathrm{s+c},k}]}, \tag{8}$$

for node k, measured in decibel (dB), where $E[D_{\mathrm{s+c},k}]$ represents the expected video distortion given in Eq. (7). Obviously, higher values of the utility function correspond to better quality of the video that reaches the end–user.

A *feasible set*, $\mathbf{U}$, is the set of all possible resource allocation scenarios that satisfy all problem constraints. In our problem, it is the vector comprised by the utilities of all K nodes, defined as:

$$\mathbf{U} = (U_1, U_2, \ldots, U_K)^\top,$$

where the utility for each node results from a different combination of the source coding rates, channel coding rates and transmission powers of the nodes.

Typically, a feasible set $\mathbf{U}$ shall satisfy conditions such as convexity, closedness and being upper–bounded. Also, it has to allow free disposal,[13] i.e., each player is permitted to dispose of utility, at will. In the case of video, this means that a node can purposely add noise to its video to degrade video quality. Despite the fact that this is obviously not a wise choice on behalf of the players, we should not restrict their possible choices regarding the way of dividing resources, except for the cases that these distributions are impossible to be implemented.

A node, in order to show readiness for joining the game, has to ensure a guaranteed minimum utility, which would not be further reduced in any case, even if game negotiations break down. The vector of minimum achievable utilities that all nodes expect by joining the game, even in case of negotiations failure, is called the *disagreement point*:

$$dp = (dp_1, dp_2, \ldots, dp_K)^\top,$$

and it shall belong to the feasible set. This point captures the minimum utility that corresponds to the minimum acceptable PSNR for each node k. In our work, dp is strictly imposed by the designer of the system.

Another interesting notion that needs to be mentioned is that of *Pareto–optimality*. An outcome of a game is Pareto–optimal if there is no other outcome that favors all players at the same time. Such an outcome is an element of the feasible set, which corresponds to a resource distribution rule and incurs an increase to the utility of each node at the same time. All Pareto–optimal points are points of the feasible set and assign to all nodes a utility that is at least as high as it is at the disagreement point. The *bargaining set* includes all Pareto–optimal points and, thus, it is a subset of the feasible set.

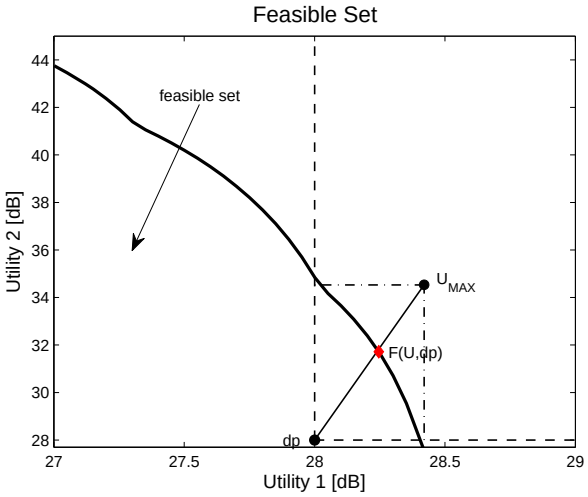

Figure 1. A feasible set and the KSBS.

6. KALAI–SMORODINSKY BARGAINING SOLUTION

As previously mentioned, convexity is one of the conditions that a feasible set has to satisfy. However, for the KSBS, the feasible set does not necessarily need to be convex, but it need to be at least *comprehensive*.[5] By definition, a set $\mathbf{U} \subset \mathbb{R}^n$ is comprehensive if, given a point $z \in \mathbb{R}^n$, the relation $z \leqslant x \leqslant y$ with $y \in \mathbf{U}$, implies $x \in \mathbf{U}$. Allowing *free disposal* for the feasible set, i.e., permitting each player to dispose of utility at will, clearly implies that the feasible set $\mathbf{U}$ is comprehensive.[5]

The Kalai–Smorodinsky bargaining solution $F(\mathbf{U}, dp)$, for the feasible set $\mathbf{U}$ and disagreement point dp, is the solution that satisfies the following properties:[5,13]

(1) $F(\mathbf{U}, dp) \geqslant dp$.

(2) $y \gg F(\mathbf{U}, dp) \Rightarrow y \notin \mathbf{U}$.

(3) Given any strictly increasing affine transformation $\tau()$, it holds that $F(\tau(\mathbf{U}), \tau(dp)) = \tau(F(\mathbf{U}, dp))$.

(4) Suppose that $dp \in \mathbf{U}' \subseteq \mathbf{U}$ and U_{MAX} is identical for both $(\mathbf{U}, dp)$ and $(\mathbf{U}', dp)$. Then, if $F(\mathbf{U}', dp)$ is a Pareto–optimal point of $\mathbf{U}$, it holds that $F(\mathbf{U}, dp) = F(\mathbf{U}', dp)$.

The quantity U_{MAX}, called the *utopian point*,[5] is the vector of maximum achievable utilities that each node can get by joining the game and it is formally defined as:

$$U_{\mathrm{MAX}}(\mathbf{U}, dp) = \left(\max_{U_1 \in \mathbf{U}} U_1, \max_{U_2 \in \mathbf{U}} U_2, \ldots, \max_{U_K \in \mathbf{U}} U_K \right)^{\top} \geqslant dp,$$

where $\max U_k$ represents the maximum possible utility for node k and shall be greater or equal to the utility at its disagreement point dp_k. Usually, all nodes cannot simultaneously achieve their maximum possible utility, hence the utopian point does not belong to the feasible set.

Annotating the Kalai–Smorodinsky bargaining solution's properties, the first two state that the bargaining solution lies in the bargaining set, while the third one stipulates that if the utility function or the disagreement point are scaled by an affine transformation, the bargaining solution remains unaffected. The last property, called *individual monotonicity*, presents the circumstances under which two sets have the same solution.

Since axiomatic bargaining theory is rather descriptive, in our study we followed an equivalent geometric approach to obtain the KSBS. Specifically, we considered that the KSBS is found by taking the maximal element

of the feasible set on the line connecting the disagreement point and the utopian point. For this purpose, we first have to determine the feasible set $\mathbf{U}$ that includes the points resulting from all different combinations of the source coding rates, channel coding rates, and transmission powers. Next, we define the disagreement point dp and find the utopian point U_{MAX} that has as coordinates the maximum possible utilities of all nodes. In the following, we simply connect dp and U_{MAX} with a straight line, and compute the equation of the straight line. Having calculated the bargaining set, which consists of the union of all Pareto–optimal points, we approximate the curve that characterizes the above set. Thus, having a system of two equations (these of the straight line and curve), we solve this system and obtain the KSBS $F(\mathbf{U}, dp)$ as the intersection point. See for example Fig. 1.

7. NODE CLUSTERING

This work considers that the nodes of the network are spatially distributed so as to cover a large area, gathering data from different fields of view. Therefore, it is reasonable for the video captured by each node to have its own video content characteristics. In view of the computational cost that increases under this assumption, we relaxed this limitation by considering that the K nodes of the network are grouped into M motion classes based on the amounts of the detected motion in each captured video.

In particular, we clustered the nodes into $M = 2$ motion classes, considering that the videos imaged by all nodes include either high or low levels of motion. Consequently, a high–motion class of nodes, including nodes that image high levels of motion, and a low–motion class of nodes, including nodes that image relatively stationary fields, were considered. Adopting this classification, the vectors that were finally needed to be determined in order to calculate the expected video distortion for each class of nodes, as given in Eq. (7), were:

$$S = (S_{\mathrm{h}}, S_{\mathrm{l}})^{\top}, \qquad R_{\mathrm{s+c,h}} = (R_{\mathrm{s,h}}, R_{\mathrm{c,h}})^{\top}, \qquad R_{\mathrm{s+c,l}} = (R_{\mathrm{s,l}}, R_{\mathrm{c,l}})^{\top},$$

where S is the vector of transmission powers of the two motion classes, while $R_{\mathrm{s+c,h}}$, and $R_{\mathrm{s+c,l}}$ are the vectors of the combinations of source–channel coding rates for the high–motion and low–motion class of nodes, respectively. Evidently, in cases where the levels of motion in the captured scenes change, e.g., the stillness of a forest is disturbed by the passage of an animal, then a new classification of the nodes is required, thereby implying a new resource allocation problem.

8. SYSTEM SETUP AND EXPERIMENTAL RESULTS

Having assumed node clustering in two motion classes, we considered two video sequences in order to represent each motion level. Therefore, we used the "Foreman" and "Akiyo" video sequences at quarter common intermediate format (QCIF) resolution for the high–motion and low–motion class of nodes, respectively, while we considered a total of $K = 100$ nodes in the network. Consequently, it was necessary to use two sets of URDC, one for each motion class, while the characteristics for the aforementioned video sequences were obtained at a frame rate of 15 frames–per–second (fps). For the calculation of the parameters α and β of Eq. (7), we corrupted each video bit stream with packet errors, assuming a bit error rate of $P_{\mathrm{b}} = 10^{-7}, 10^{-6}$, and 10^{-5}. The employed modulation scheme was the binary phase shift keying and, for the RCPC codes, the mother code rate was $1/4$.[12]

Regarding the bandwidth, W_t, we used the values of 20 MHz and 15 MHz, and the considered bit rate constraint was 96 kbps. As it was also mentioned in Section 3, the restriction of channel coding rates to discrete values,[12] results in discrete values also for the source coding rates (see Eq. (2)). Thus, the corresponding source–channel coding rate combinations for each motion class regarding the above bit rate constraint were:

$$\Big\{(32\,\mathrm{kbps}, 1/3), (48\,\mathrm{kbps}, 1/2), (64\,\mathrm{kbps}, 2/3)\Big\}.$$

The transmission powers were allowed to take continuous values in the range $\mathbf{S} = [5, 15]$ Watts. In an effort to reduce the infinite number of points of the feasible set that result from all possible combinations of the source coding rates, channel coding rates and transmission powers (with infinite decimal digits), we assumed that the transmission powers can take values within the above set, with a step size equal to 10^{-1}:

$$\Big\{S_{\mathrm{h}}, S_{\mathrm{l}}\Big\} \in \Big\{5.0,\ 5.1,\ 5.2, \ldots, 14.8,\ 14.9,\ 15.0\Big\}.$$

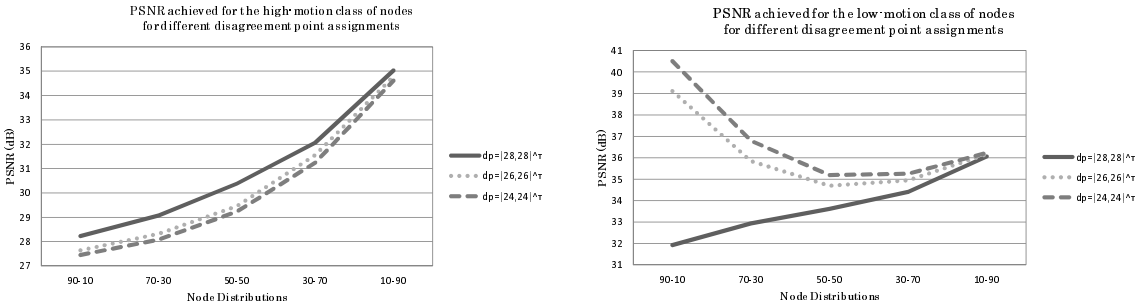

(a) (b)

Figure 2. PSNR values for different assignments to the disagreement point (a) for the high–motion, and (b) for the low–motion class of nodes, for various node distributions with $R_k = 96$ kbps and $W_t = 20$ MHz.

Node Distribution	$(R_{\mathrm{s,h}}, R_{\mathrm{c,h}})$	S_{h}	$(R_{\mathrm{s,l}}, R_{\mathrm{c,l}})$	S_{l}	$PSNR_{\mathrm{h}}$	$PSNR_{\mathrm{l}}$
$90-10$	$(48\,\mathrm{kbps}, 1/2)$	12.8	$(32\,\mathrm{kbps}, 1/3)$	7.0	28.2331	31.9265
$70-30$	$(48\,\mathrm{kbps}, 1/2)$	13.4	$(32\,\mathrm{kbps}, 1/3)$	7.5	29.0743	32.9283
$50-50$	$(64\,\mathrm{kbps}, 2/3)$	11.8	$(32\,\mathrm{kbps}, 1/3)$	6.4	30.3871	33.6159
$30-70$	$(64\,\mathrm{kbps}, 2/3)$	12.2	$(32\,\mathrm{kbps}, 1/3)$	6.3	32.0676	34.4021
$10-90$	$(64\,\mathrm{kbps}, 2/3)$	14.8	$(64\,\mathrm{kbps}, 2/3)$	6.2	35.0234	36.0588

Table 1. KSBS for various node distributions with $R_k = 96\,\mathrm{kbps}$, $W_t = 20\,\mathrm{MHz}$ and $dp = (28, 28)^\top$ dB.

Node Distribution	$(R_{\mathrm{s,h}}, R_{\mathrm{c,h}})$	S_{h}	$(R_{\mathrm{s,l}}, R_{\mathrm{c,l}})$	S_{l}	$PSNR_{\mathrm{h}}$	$PSNR_{\mathrm{l}}$
$90-10$	$(32\,\mathrm{kbps}, 1/3)$	12.0	$(32\,\mathrm{kbps}, 1/3)$	10.9	26.3116	33.4576
$70-30$	$(32\,\mathrm{kbps}, 1/3)$	7.4	$(32\,\mathrm{kbps}, 1/3)$	5.0	26.7383	31.7640
$50-50$	$(48\,\mathrm{kbps}, 1/2)$	13.4	$(32\,\mathrm{kbps}, 1/3)$	7.0	27.6905	30.9606
$30-70$	$(64\,\mathrm{kbps}, 2/3)$	11.2	$(32\,\mathrm{kbps}, 1/3)$	5.1	29.6223	31.6116
$10-90$	$(64\,\mathrm{kbps}, 2/3)$	12.7	$(32\,\mathrm{kbps}, 1/3)$	5.0	32.9874	33.0089

Table 2. KSBS for various node distributions with $R_k = 96\,\mathrm{kbps}$, $W_t = 15\,\mathrm{MHz}$ and $dp = (26, 26)^\top$ dB.

As mentioned in Section 5, the disagreement point's value in this work is imposed by the designer of the system. Trying to arrive at an appropriate assignment for this amount, we experimented with different values. Specifically, the tested values per bit rate–bandwidth combination were:

(1) $R_k = 96$ kbps, $W_t = 20$ MHz and for dp we considered:

(a) $dp = (28, 28)^\top$ dB,

(b) $dp = (26, 26)^\top$ dB,

(c) $dp = (24, 24)^\top$ dB.

(2) $R_k = 96$ kbps, $W_t = 15$ MHz and for dp we considered:

(a) $dp = (26, 26)^\top$ dB,

(b) $dp = (25, 25)^\top$ dB,

(c) $dp = (24, 24)^\top$ dB.

The values that were finally selected were $dp = (28, 28)^\top$ dB for the first case, and $dp = (26, 26)^\top$ dB for the second case. Figure 2 presents the PSNR values achieved for each of the above assignments to the disagreement point, both for the high– (Fig. 2(a)) and low–motion (Fig. 2(b)) class of nodes, for the case of $R_k = 96$ kbps and

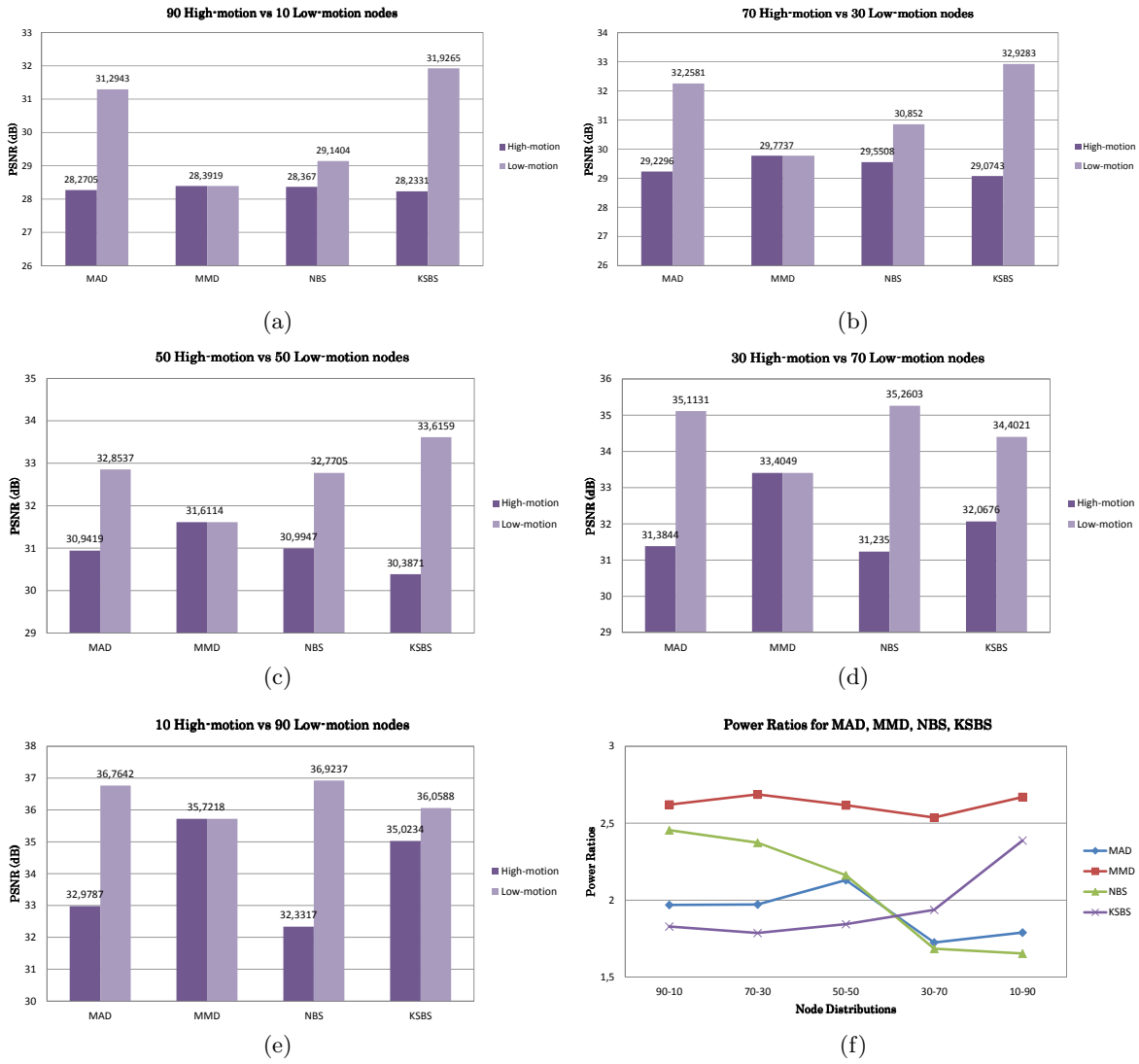

Figure 3. (a)–(e) Comparison of the PSNR values for the high– and low–motion class of nodes. (f) Comparison of the power ratios for the MAD, MMD, NBS and KSBS criteria, for various node distributions with $R_k = 96$ kbps, $W_t = 20$ MHz and $dp = (28, 28)^\top$ dB.

$W_t = 20$ MHz. Also, the same figure illustrates how these values vary as the number of nodes of the high–motion class reduces while that of the low–motion one increases. The term "Node Distributions" refers to the numbers of nodes in the high– and low–motion class of nodes, respectively.

Tables 1 and 2 report the aggregated results regarding the KSBS criterion, solely. Specifically, Table 1 refers to the case of $R_k = 96$ kbps and $W_t = 20$ MHz, while Table 2 refers to $R_k = 96$ kbps and $W_t = 15$ MHz. The pair $(R_{\mathrm{s,h}}, R_{\mathrm{c,h}})$ denotes the combination of the source–channel coding rate of the high–motion class of nodes, while S_{h} and $PSNR_{\mathrm{h}}$ denote the transmission power and the PSNR of the aforementioned motion class, respectively. The corresponding parameters for the low–motion class are denoted as $(R_{\mathrm{s,l}}, R_{\mathrm{c,l}})$, S_{l} and $PSNR_{\mathrm{l}}$, respectively.

An in–depth look at the provided results led us to some useful observations. Starting with Fig. 1, we observed that the feasible set was marginally non–convex when $R_k = 96$ kbps, $W_t = 20$ MHz and $dp = (28, 28)^\top$ dB, for 90 nodes belonging to the high–motion class and 10 nodes belonging to the low–motion class. The "Foreman" video sequence represents the high–motion class and the "Akiyo" video sequence the low–motion class. Nevertheless, the feasible set was unique for specific video sequences, node distributions (number of nodes per motion class)

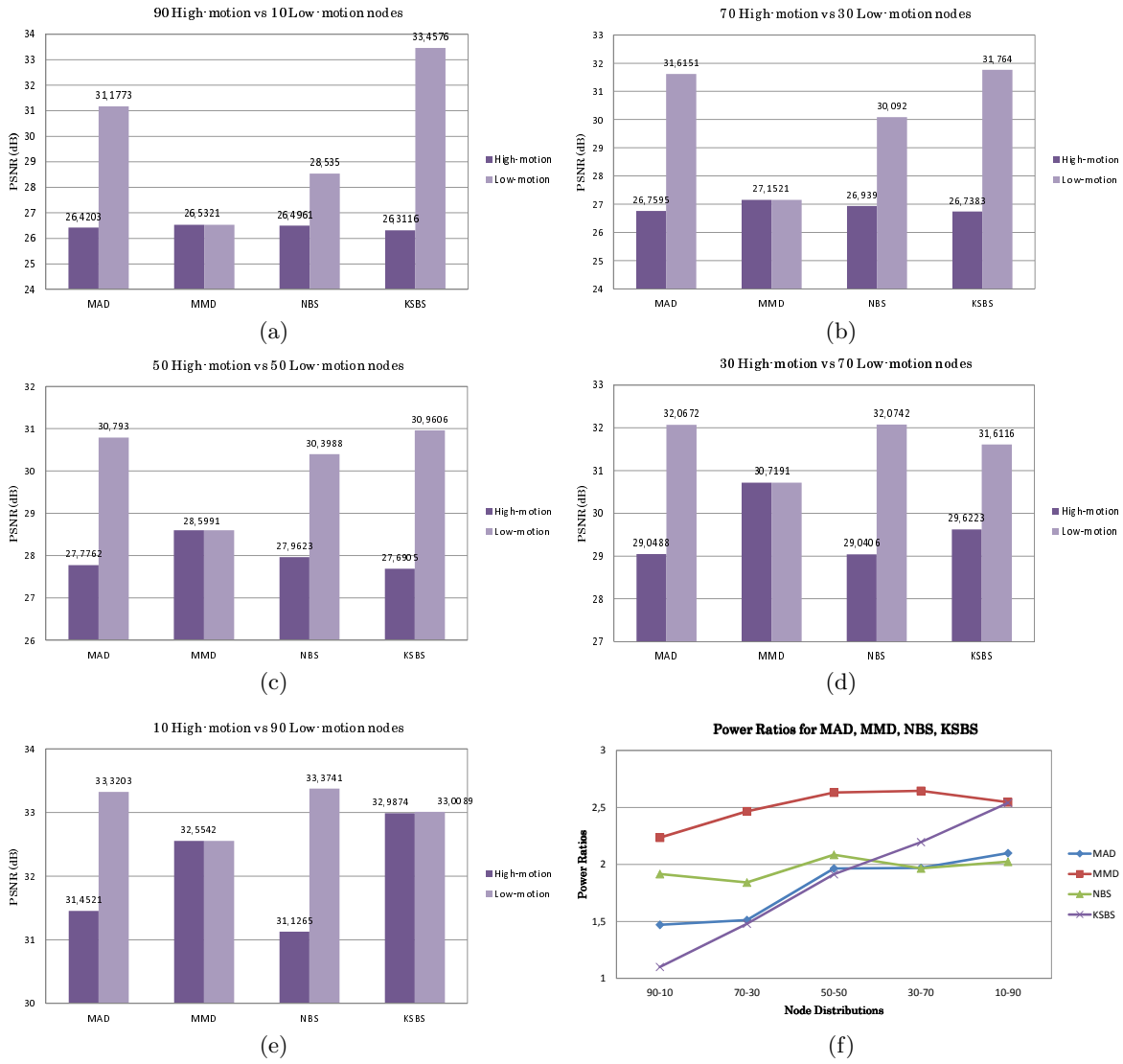

Figure 4. (a)–(e) Comparison of the PSNR values for the high– and low–motion class of nodes. (f) Comparison of the power ratios for the MAD, MMD, NBS and KSBS criteria, for various node distributions with $R_k = 96\,\text{kbps}$, $W_t = 15\,\text{MHz}$ and $dp = (26, 26)^\top$ dB.

and parameter initializations (bit rate and bandwidth values). Having conducted a large number of experiments, we confirmed that the feasible sets examined in our study, were all marginally non–convex. However, this does not impose a problem, since they all remain comprehensive.

Passing to Fig. 2, the most interesting observation was the advantage gained by the high–motion class of nodes when disagreement point assumed higher values. The negative effect was observed for the low–motion class of nodes. This fact was verified by the achieved PSNR values for the two motion classes. It shall be underlined that in our study the selected values for the disagreement point were the highest among the considered ones for each bit rate and bandwidth combination. This choice was driven by the reasonable requirement for best possible video quality of the high–motion videos, since they usually capture more important information than videos that include relatively stationary scenes.

In addition, Fig. 2 offers another interesting observation for the case of $dp = (28, 28)^\top$ dB. Specifically, since the number of nodes of the high–motion class reduces and that of the low–motion class increases, the PSNR values for both motion classes show an increasing trend. This is in contrast to the other two disagreement point

assignments, where a reduction in the PSNR values of the low–motion class of nodes was observed.

Further investigation of the tables confirms the expectation that the low–motion class of nodes compresses the data at a lower compression rate compared to the high–motion class, using more bits for data protection through channel transmission. Therefore, this motion class can transmit data spending less power, thereby prolonging battery lifetime of battery–operated nodes. Moreover, the low–motion class of nodes was more favored by the KSBS compared to the high–motion class, as it is indicated by the corresponding PSNR values. Another noteworthy point was the reduction of PSNR values of both motion classes in Table 2, where the bit rate was equal to 96 kbps, while the bandwidth was reduced to 15 MHz from 20 MHz in Table 1. This can be attributed to the reduction incurred to the ratio of Eq. (3), which implies the necessity for lower disagreement points in order to retain their feasibility.

The performance of KSBS was also assessed against the MAD, MMD and NBS criteria, presented in previous works.[2,3] Undoubtedly, the KSBS has the comparative advantage of offering the highest levels of video quality to the low–motion videos in cases where the low–motion class of nodes consists of fewer nodes than the high–motion class, while minimizing its power consumption. On the contrary, in cases where the low–motion class of nodes has lower cardinality than the high–motion class, the videos that include high levels of motion achieve significantly increased video quality with the KSBS, while the visual quality of the low–motion class is further improved. In such cases, although the power ratios of the KSBS are higher compared to MAD and NBS, it assures the highest pairs of PSNR values for the two motion classes compared to all the other approaches.

9. CONCLUSIONS

Summarizing our results, the KSBS is the best choice if we are interested in maximizing the video quality of low–motion videos. Also, it remains a promising choice for improving the quality of high–motion videos, especially when the low–motion class contains more nodes than the high–motion one. The proposed method does not require high levels of power to transmit the data through the network. Moreover, it has low running complexity, since the solution is graphically derived for each feasible set. In general, our observations are in line with the general feeling that the most appropriate approach for tackling resource allocation problems in wireless DS–CDMA VSN is rather problem–dependent, since it always depends on the application's special characteristics and requirements.

ACKNOWLEDGEMENT

This research was supported by a Marie Curie International Reintegration Grant within the 7th European Community Framework Programme.

REFERENCES

[1] Bentley, E. S., Kondi, L. P., Matyjas, J. D., Medley, M. J., and Suter, B. W., "Spread spectrum visual sensor network resource management using an end–to–end cross–layer design," *IEEE Transactions on Multimedia* **13**, 125–131 (Feb. 2011).

[2] Pandremmenou, K., Kondi, L. P., and Parsopoulos, K. E., "Optimal power allocation and joint source–channel coding for wireless DS–CDMA visual sensor networks," in [*Proc. SPIE Electronic Imaging Symposium*], (Jan. 2011). SPIE Vol. 7882, Article 788206.

[3] Pandremmenou, K., Kondi, L. P., and Parsopoulos, K. E., "Optimal power allocation and joint source–channel coding for wireless DS–CDMA visual sensor networks using the Nash bargaining solution," in [*36th International Conference on Acoustics, Speech and Signal Processing*], 2340–2343 (May 2011).

[4] Kalai, E. and Smorodinsky, M., "Other solutions to Nash's bargaining problem," *Econometrica* **43**(3), 513–518 (1975).

[5] Conley, J. P. and Wilkie, S., "The bargaining problem without convexity: extending the Egalitarian and Kalai–Smorodinsky solutions," *Economic Lett.* **36**, 365–369 (Aug. 1991).

[6] Khan, M. A., Truong, C., Geithner, T., Sivrikaya, F., and Albayrak, S., "Network level cooperation for resource allocation in future wireless networks," in [*Wireless Days, 2008. WD '08. 1st IFIP*], 1–5 (Nov. 2008).

[7] Yang, B., Shen, Y., Feng, G., and Guan, X., "Fair resource allocation using bargaining over OFDMA relay networks," in [*CDC*], 585–590 (2009).

[8] Chen, J. and Swindlehurst, A. L., "Downlink resource allocation for multi–user MIMO–OFDMA systems: The Kalai–Smorodinsky bargaining approach," in [*3rd IEEE International Workshop on Computational Advances in Multi–Sensor Adaptive Processing (CAMSAP)*], 380–383 (Dec. 2009).

[9] Park, H. and van der Schaar, M., "Fairness strategies for wireless resource allocation among autonomous multimedia users," *IEEE Transactions on Circuits and Systems for Video Technology* **20**, 297 –309 (Feb. 2010).

[10] Park, H. and van der Schaar, M., "Fairness strategies for multi–user multimedia applications in competitive environments using the Kalai–Smorodinsky bargaining solution," in [*Proc. IEEE International Conference on Acoustics, Speech and Signal Processing*], (2007).

[11] Mastronarde, N. and van der Schaar, M., "A bargaining theoretic approach to quality–fair system resource allocation for multiple decoding tasks," *IEEE Transactions on Circuits and Systems for Video Technology* **18**, 453–466 (Apr. 2008).

[12] Hagenauer, J., "Rate–compatible punctured convolutional codes (RCPC codes) and their applications," *IEEE Transactions on Communications* **36**, 389–400 (Apr. 1988).

[13] Binmore, K., [*Playing for Real: A Text on Game Theory*], Oxford University Press (2007).